Conclusion

The appearance of instabilities resultant from coalescence of neighboring jets has been observed and confirmed for flow through porous plates. This flow instability appears similar to those previously reported by Morgan[2] and Bradshaw.[5] A critical velocity exists, above which instabilities appear. This critical velocity depends on the plate porosity. The presence of a shear flow over the plate seems to stabilize the jets. No effect was observed in heat-transfer measurements with transpiration.

References

[1] MacPhail, D., ARC R & M 1876, 1939, Aeronautical Research Council, London, England.

[2] Morgan, P. G., "The Stability of Flow Through Porous Screens," *Journal of the Royal Aeronautical Society*, Vol. 64, 1960, pp. 359–362.

[3] von Bohl, D., *Ingenieur Archiv*, Vol. 11, No. 4, 1940, p. 295.

[4] Corrsin, S., ACR 2H24, 1944, NACA.

[5] Bradshaw, P., "The Effect of Wind-Tunnel Screens on Nominally Two-Dimensional Boundary Layers," *Journal of Fluid Mechanics*, Vol. 22, Pt. 3, 1965, pp. 679–687.

[6] Schubauer, G. M., *Journal of the Aeronautical Sciences*, Vol. 14, 1947, p. 4.

[7] Moffat, R. J. and Kays, W. M., "The Turbulent Boundary Layer and Porous Plate: Experimental Heat Transfer with Uniform Blowing and Suction," Rept. HMT-1, 1967, Thermosciences Div., Dept. of Mechanical Engineering, Stanford University, Stanford, Calif.

Flowfield in the Combustion Chamber of a Solid Propellant Rocket Motor

R. DUNLAP,* P. G. WILLOUGHBY,† AND R. W. HERMSEN‡
United Technology Center, Sunnyvale, Calif.

Introduction

An accurate description of the three-dimensional flowfield in a rocket chamber is required in order to develop further understanding and more precise prediction techniques in areas such as metal combustion, metal oxide particle growth, erosive propellant burning, and damping of acoustic waves. In connection with the acoustic damping problem, Culick[1] presented an analytical solution for the steady, inviscid, incompressible flow in an internal-burning cylindrical grain configuration wherein the fluid was assumed to enter normal to the burning surface. This flow has the interesting feature that while satisfying the inviscid equations of motion it also satisfies the no-slip boundary condition of a viscous fluid. In this Note it is shown that this same velocity field also closely satisfies the viscous equations of motion, except in a small region near the head-end of the chamber. The expectation that the Culick solution may therefore accurately represent the real flow was verified by an experiment carried out in a porous tube apparatus.

Applicability of Inviscid No-Slip Solution to Actual Flow

The solution derived by Culick,[1] for the motion of an incompressible and inviscid fluid entering at a uniform rate normal to the wall of a circular cylinder which is closed at $z = 0$, may be written

$$u(r,z) = v_w \pi (z/r_w)\cos(\pi r^2/2r_w{}^2) \quad (1)$$

$$v(r,z) = (-v_w r_w/r)\sin(\pi r^2/2r_w{}^2) \quad (2)$$

$$P(r,z) = P(o,o) - (\rho/2)[v^2(r,z)+u^2(o,z)] \quad (3)$$

where P is the pressure, u and v are the velocity components in the z and r directions, respectively, and v_w is the magnitude of the wall velocity. Since this flow satisfies the viscous no-slip condition along the boundary $r = r_w$, the question arose as to what degree it may represent the entire viscous flowfield. To be an accurate solution to the viscous equations of motion, the flow represented by Eqs. (1–3) must also satisfy the condition that the net viscous force acting on a fluid element is small compared to the net pressure force. That is, in this event the flow satisfies both the inviscid and viscous equations of motion while also satisfying the no-slip boundary condition.

The ratio of magnitudes of the differential viscous force on a fluid element to the differential pressure force for this flowfield may be written

$$FR = \frac{|\text{net viscous force}|}{|\text{net pressure force}|} = \mu \left\{ \frac{\left[\frac{\partial^2 u}{\partial r^2} + \frac{\partial^2 u}{\partial z^2} + \frac{1}{r}\frac{\partial u}{\partial r}\right]^2 + \left[\frac{\partial^2 v}{\partial z^2} + \frac{\partial^2 v}{\partial r^2} + \frac{\partial}{\partial r}\left(\frac{v}{r}\right)\right]^2}{\left(\frac{\partial P}{\partial z}\right)^2 + \left(\frac{\partial P}{\partial r}\right)^2} \right\}^{1/2} =$$

$$\frac{4}{Re}\left\{ \frac{\left[\sin\left(\frac{\pi r^2}{2r_w{}^2}\right) + \frac{\pi r^2}{2r_w{}^2}\cos\left(\frac{\pi r^2}{2r_w{}^2}\right)\right]^2 + \frac{r^2}{4z^2}\sin^2\left(\frac{\pi r^2}{2r_w{}^2}\right)}{1 + \frac{r_w{}^8 \sin^2 \pi r^2/2r_w{}^2}{\pi^4 z^2 r^6}\left[\frac{r^2\pi}{r_w{}^2}\cos\left(\frac{\pi r^2}{2r_w{}^2}\right) - \sin\left(\frac{\pi r^2}{2r_w{}^2}\right)\right]^2} \right\}^{1/2}$$

where $Re = 2\rho v_w r_w/\mu$ is the Reynolds number. This ratio satisfies the inequality

$$FR < \frac{5.56}{Re}\left(1 + \frac{r^2}{7.72z^2}\right)^{1/2}$$

Thus, when the Reynolds number is large the viscous stresses are indeed negligible compared to pressure forces except in the narrow region $z/r = 0(1/Re)$ at the head end of the chamber.

In concluding that Eqs. (1–3) closely represent the actual flow in a rocket chamber, where Re is the order of 10^4 to 10^5, it should be emphasized that the abovementioned arguments are based on the assumption of laminar flow. However, the same conclusion would be reached for turbulent flow with this velocity distribution as long as the net force due to Reynolds stress acting on a fluid element is small compared to the net pressure force.

Experiment to Determine Chamber Flowfield

To test the above reasoning, as well as possible implications of turbulence, a cold flow experiment was devised in which a series of five cylindrical porous tubes were used to simulate the propellant surface (see Fig. 1). The porous tubes were sintered bronze having a wall thickness of 0.10 in. and a pore size in the range 5–15 μ. Ambient temperature nitrogen entered the chamber uniformly through the porous tubes and exited to the atmosphere through an aluminum section which joined smoothly to the last porous tube. Centerline velocity distributions were measured with a hot-wire anemometer made from 0.00035-in. by 0.10-in.

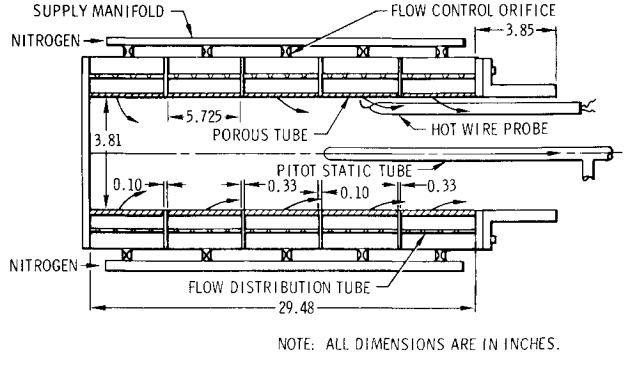

Fig. 1 Experimental apparatus for cold flow simulation of rocket chamber flowfield.

Received March 29, 1974.

Index categories: Nozzle and Channel Flow; Viscous Nonboundary-Layer Flows; Solid and Hybrid Rocket Engines.

* Senior Staff Scientist. Member AIAA.

† Senior Scientist.

‡ Manager, Physical Sciences Laboratory. Associate Fellow AIAA.

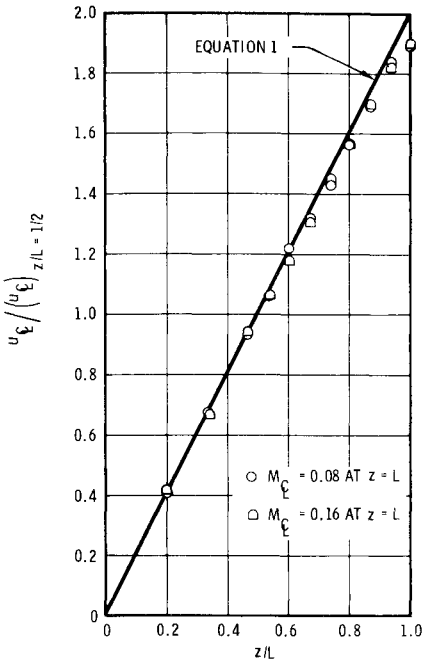

Fig. 2 Centerline velocity distribution.

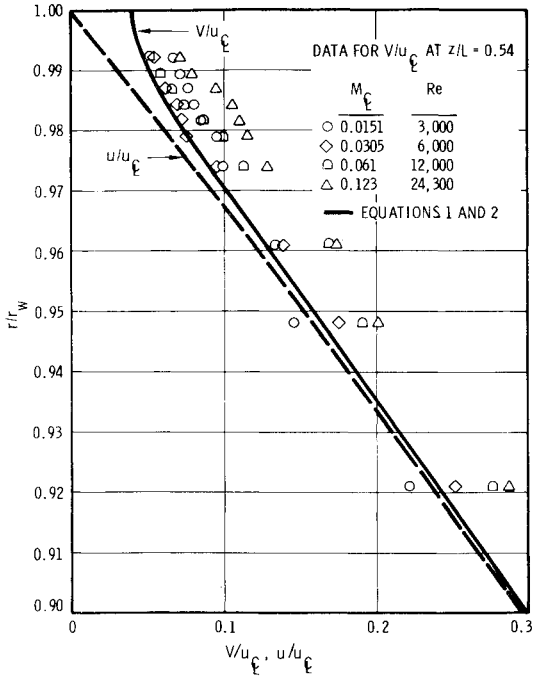

Fig. 4 Radial distribution of velocity near the wall.

manometer. The radial distribution of the mean and fluctuating components of velocity were measured at a fixed axial location with a hot-wire anemometer made from 0.0035-in. by 0.10-in. tungsten. The wire was connected to an automatic bridge circuit which maintained a constant wire overheat ratio of 0.667. Wire voltage fluctuations were measured with a Ballantine true rms meter. Positioning of the wire was accomplished with a traveling micrometer screw and the surface location was determined by electrical contact.

Results and Discussion

The centerline velocity distribution, relative to the value at $z/L = \frac{1}{2}$, is shown in Fig. 2 together with the linear behavior predicted by Eq. (1). The data show reasonable agreement with the theory except for an end effect which appears to propagate upstream somewhat beyond the last porous tube. This result, while in agreement with the theory, does not provide a direct check since velocity profiles of any radial distribution would produce a linear acceleration as long as they were similar at each axial station.

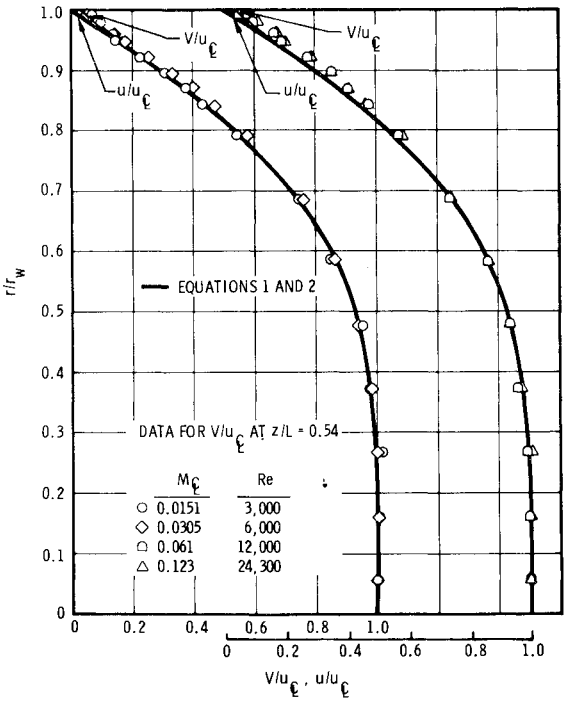

Fig. 3 Radial distribution of velocity at $z/L = 0.54$.

Radial distributions of the velocity vector magnitude V measured at $z/L = 0.54$ are shown in Figs. 3 and 4 for four values of Reynolds number. Also shown are the theoretical curves for V/u_C and u/u_C predicted from Eqs. (1) and (2). In general, there is excellent agreement between measurements and theory, thus verifying the applicability of the inviscid fluid solution to the real flow.

As discussed previously, this agreement was anticipated for laminar flow and also for turbulent flow as long as the net force due to Reynolds stress on a fluid element is small compared to the net pressure force. Measurements of the velocity fluctuation level at each of the points in Figs. 3 and 4 showed a fair degree of turbulence in the flow. The rms value of the fluctuating velocity in the direction of the mean flow, divided by the local mean speed, increased from 0.02 at the centerline to a maximum of 0.04 at $r/r_w = 0.99$, when the Reynolds number was 3000. The corresponding variation in turbulence level for $Re =$ 24,000 was from 0.015 at the centerline to 0.15 at $r/r_w = 0.99$. This level of turbulence is of similar magnitude to that measured for fully developed pipe flow[2] where the net viscous and Reynolds stresses acting on a fluid element are in equilibrium with the differential pressure stresses. However, for the present accelerating flow the agreement between experiment and theory implies that the net force due to Reynolds stress, as well as viscous stress, is negligible compared to pressure force. The Reynolds stress, $\rho\overline{u'v'}$, was not measured in these experiments so the ratio of turbulent shear force, $r^{-1}\partial(r\rho\overline{u'v'})/\partial r$, to net pressure, $\partial P/\partial z$, could not be checked directly. Calculations based on the measured $\overline{u'^2}$ distributions showed that $r^{-1}\partial(\rho r\overline{u'^2})/\partial r \div \partial P/\partial z$ was typically less than 0.05. Thus, if $\partial(r\overline{u'v'})/\partial r$ is less than or of the same order as $\partial(r\overline{u'^2})/\partial r$, as with fully developed pipe flow,§ the present turbulence level data would also confirm the relative unimportance of Reynolds stresses in the flowfield.

§ Examination of data[2] for fully developed pipe flow indicates that $\partial(r\overline{u'v'})/\partial r < \frac{1}{3}\partial(r\overline{u'^2})/\partial r$ for $0.1 < r/r_w < 0.9$.

References

[1] Culick, F. E. C., "Rotational Axisymmetric Mean Flow and Damping of Acoustic Waves in a Solid Propellant Rocket," *AIAA Journal*, Vol. 4, No. 8, Aug. 1966, pp. 1462–1464.

[2] Hinze, J. O., *Turbulence*, McGraw-Hill, New York, 1959, pp. 521–525.

Equations of Motion for the Perturbed Restricted Three-Body Problem

T. A. HEPPENHEIMER*
California Institute of Technology, Pasadena, Calif.

BROWN and Shook[1] discussed a particular case of the perturbed restricted problem in their treatment of the motion of the Trojan asteroids. But they did not give a general method for the perturbed restricted problem. Farquhar[2] has given such general equations of motion. In the unperturbed circular problem, one normalizes to unity the (constant) distance between primaries r, their mean motion $\dot{\theta}$, and the sum of their masses. The smaller primary is of mass μ. Also, the coordinate system (x, y, z) rotates with angular velocity $\dot{\theta}$, such that the locations of masses μ, $1-\mu$ are, respectively, $x_1 = -(1-\mu)$, $x_2 = \mu$. To incorporate the indirect effect in the perturbed case, Farquhar has

$$r = 1+\rho(t), \quad \dot{\theta} = 1+v(t) \tag{1}$$

so that the primaries are at $x_1 = -(1-\mu)(1+\rho)$, $x_2 = \mu(1+\rho)$. Then, the equations of motion are given relative to the barycenter; the independent variable is the mean anomaly l

$$\begin{aligned}
&\ddot{x}-2(1+v)\dot{y}-\dot{v}y-(1+v)^2x+\frac{1-\mu}{r_1^3}[x-\mu(1-\rho)]+\\
&\qquad\frac{\mu}{r_2^3}[x+(1-\mu)(1+\rho)] = V_x\\
&\ddot{y}+2(1+v)\dot{x}+\dot{v}x-(1+v)^2y+y\left(\frac{1-\mu}{r_1^3}+\frac{\mu}{r_2^3}\right) = V_y\\
&\ddot{z}+z\left(\frac{1-\mu}{r_1^3}+\frac{\mu}{r_2^3}\right) = V_z
\end{aligned} \tag{2}$$

where $r_1^2 = [x-\mu(1+\rho)]^2+y^2+z^2$, $r_2^2 = [x+(1-\mu)(1+\rho)]^2+y^2+z^2$, and V_x, V_y, V_z are components of perturbing acceleration on the third body (direct effect).

The indirect effect then is incorporated through the perturbation quantities ρ, v, by means of the equations

$$\ddot{r}-r\dot{\theta}^2 = -r^{-2}+\partial R/\partial r; \qquad r\ddot{\theta}+2\dot{r}\dot{\theta} = (1/r)\partial R/\partial\theta \tag{3}$$

where R is the disturbing function on the motion of the primaries. Thus, it is necessary to integrate Eqs. (3), i.e., to solve analytically a perturbed two-body problem, in order to exhibit complete equations of motion for the perturbed problem. Moreover, even in the absence of perturbations, the effects of eccentric orbits of the primaries appear in Eqs. (2) as-if they were perturbations. Thus, it is of interest whether the solution of Eqs. (3) can be avoided, in deriving equations of motion.

An alternate approach follows from the derivation of equations of motion for the elliptic restricted problem by means of the Nechvile transformation.[3] In this derivation, the equations of motion in siderial coordinates are transformed and exhibit explicitly the left-hand sides of Eqs. (3) [see Eq. (61), p. 592 of Ref. 3]. Thus, let coordinates ξ, η, ζ be normalized with respect to variable r, f = true anomaly is the independent variable, $\tilde{r}_j^2 = (\xi-\xi_j)^2+\eta^2+\zeta^2$, $j = 1, 2$, and $\xi_1 = -(1-\mu)$, $\xi_2 = \mu$. Also, α is defined by

$$r(df/dl)^2 = (1+\alpha)(1+e\cos f)/r^2 = (1+e\cos f)/r^2+ 2(1+e\cos f)^{1/2}[\int(\partial R/\partial\theta)\,dl]/r^{5/2}+[\int(\partial R/\partial\theta)\,dl]^2/r^3$$

and the equations then are given

$$\begin{aligned}
&\xi''-2\eta'-[(1+\alpha)(1+e\cos f)]^{-1}\left[\xi\left(1-r^2\frac{\partial R}{\partial r}\right)-\right.\\
&\left.\frac{(1-\mu)(\xi-\mu)}{\tilde{r}_1^3}-\frac{\mu(\xi+1-\mu)}{\tilde{r}_2^3}-(\xi'+\eta)r\frac{\partial R}{\partial\theta}\right] =\\
&\qquad V_\xi\cdot r^2[(1+\alpha)(1+e\cos f)]^{-1}\\
&\eta''+2\xi'-[(1+\alpha)(1+e\cos f)]^{-1}\left[\eta\left(1-r^2\frac{\partial R}{\partial r}-\frac{1-\mu}{\tilde{r}_1^3}-\frac{\mu}{\tilde{r}_2^3}\right)-\right.\\
&\left.(\eta'-\xi)r\frac{\partial R}{\partial\theta}\right] = V_\eta\cdot r^2[(1+\alpha)(1+e\cos f)]^{-1}\\
&\zeta''+\zeta\left[1-[(1+\alpha)(1+e\cos f)]^{-1}\left(1-r^2\frac{\partial R}{\partial r}-\frac{1-\mu}{\tilde{r}_1^3}-\frac{\mu}{\tilde{r}_2^3}\right)\right]+\\
&\qquad\zeta' r\frac{\partial R}{\partial\theta} = V_\zeta\cdot r^2[(1+\alpha)(1+e\cos f)]^{-1}
\end{aligned} \tag{4}$$

In Eqs. (4), f and r appear explicitly, as in Eq. (2). Hence, for an exact treatment, one must again solve Eqs. (3), in order to obtain complete equations of motion. In such a situation, Eqs. (2) are simpler and hence preferable to Eqs. (4). But in Eqs. (4), wherever f and r appear, they are multiplied by perturbation quantities involving e, R, or V. Hence, in an approximate treatment wherein one is willing to neglect terms of order R^2, eR, etc., f and r can be given by the usual two-body relations and solution of Eqs. (3) is not required. Also α can then be neglected. Then, in such a treatment, one can use the disturbing function directly, avoiding the need for a perturbed two-body solution in deriving equations of motion.

References

[1] Brown, E. W. and Shook, C. A., *Planetary Theory*, Cambridge University Press, Cambridge, England, 1933, Chap. IX.

[2] Farquhar, R. W., "The Control and Use of Libration-Point Satellites," TR-R 346, Sept. 1970, NASA.

[3] Szebehely, V. G., *Theory of Orbits*, Academic Press, New York, 1967, pp. 588–595.

Presented as Paper 73-144 at the AIAA 11th Aerospace Sciences Meeting, Washington, D.C., January 10–12, 1973; submitted March 20, 1974; revision received June 5, 1974.

Index category: Lunar and Interplanetary Trajectories.

* Research Fellow, Division of Geological and Planetary Sciences. Member AIAA.

Wall Shear in Strongly Retarded and Separated Compressible Turbulent Boundary Layers

M. W. RUBESIN,* J. D. MURPHY,† AND W. C. ROSE‡
NASA Ames Research Center, Moffett Field, Calif.

Nomenclature

A^+ = measure of sublayer thickness
$\bar{p}$ = mean static pressure
P^+ = dimensionless pressure gradient, $(\nu/\rho u_\tau^3)\,d\bar{p}/dx$

Received April 1, 1974.

Index category: Boundary Layers and Convective Heat Transfer—Turbulent.

* Senior Staff Scientist, Thermo- and Gas-Dynamics Division. Associate Fellow AIAA.

† Research Scientist, Aeronautics Division.

‡ Research Scientist, Aeronautics Division. Member AIAA.